Cent. Eur. For. J. 72 (2026) 217–232 DOI: 10.2478/forj-2026-0007

CENTRAL EUROPEAN Forestry Journal

ORIGINAL PAPER

An enhanced algorithm for the detection of individual trees based on airborne laser scanning data combining geometric and dendrometric rules

Ivan Sačkov*

National Forest Centre – Science and Research Division, Department of Forest Policy, Forest and Game Management, T. G. Masaryka 22, SK-96001 Zvolen, Slovakia

Abstract

Airborne laser scanning has become a well-established, consolidated, and widely used technology for individual tree detection. In this context, we have developed the geoprocessing tool xTree to allow for the detection of individual tree tops and tree crowns based on a combination of airborne laser scanning data and a priori information consisting of geometric and dendrometric rules. The primary aim of this article is to present the workflow for the detection of individual trees using the xTree tool. A detailed description, flowchart, and scheme are provided for these purposes. The additional aim is to present the performance of this workflow through a case study. The study area covered 2.8 ha of forests in Slovakia. The airborne laser scanning data reached an average density of 18 ±6 points per m^2. The ground reference data included 2,119 trees in coniferous, broadleaved, and mixed strata. The enhanced detection algorithm achieved overall correctness of 85 ±2%. The overall completeness from the tree number was 69 ±4%, and the overall completeness from the tree volume was 78 ±2%. Generally, the performance increased with the increasing proportion of coniferous trees and diameter of trees.

Key words: LiDAR; forest inventory; individual tree-detection approach

Editor: Tomáš Gergeľ

1. Introduction

Information about individual trees (e.g., height, diameter, volume, position, species, condition) represents an essential data source for sustainable forest management. This is because tree-based variables are fundamental for quantitative as well as for qualitative forest inventories at a multiscale level (Bettinger et al. 2016). In recent years, airborne laser scanning (ALS) has become a well-established, consolidated, and widely used technology for the detection of individual trees and evaluation of related information (Vauhkonen et al. 2014).

Generally, there are three groups of methods for detecting individual trees in relation to the form of ALS data: (1) elevation model-based methods (EM-based), (2) point cloud-based methods (PC-based), and (3) hybrid-based methods (H-based). These methods were last comprehensively reviewed (Zhen et al. 2016) and benchmarked (Kaartinen et al. 2012; Vauhkonen et al. 2012; Eysn et al. 2015; Wang et al. 2016) in 2016. To uncover current trends, our article therefore provides an overview of key features from the thirty most relevant studies focused on the detection of individual trees based on ALS data over the last decade (Table 1–3).

EM-based methods (Table 1) mostly use a canopy height model as a data source for the identification of individual trees. Image-filtering methods with fixed or variable window size can be used firstly to find tree tops so that image segmentation methods (e.g., watershed, region growing, tessellation) can be used to delineate tree crowns. These methods are relatively easy to use, but they usually include some smoothing procedures that significantly reduce information regarding tree crowns and the understory.

PC-based methods (Table 2) mostly use a normalized point cloud as a data source for the identification of individual trees. Point cloud-clustering methods (e.g., k-means, k-nearest, mean-shift) can be used to identify tree tops and tree crowns. These methods are usually computationally intensive, but they take into account most of the information from the entire 3D structure of the data source.

*Corresponding author. Ivan Sačkov, e-mail: ivan.sackov@nlcsk.org
© 2026 Authors. This is an open access article under the CC BY 4.0 license.

H-based methods (Table 3) use various combinations of elevation models, point clouds, other geospatial data sources (e.g., aerial images), and specific a priori information (e.g., vertical or horizontal attributes of trees). These methods represent an efficient trade-off between EM-based and PC-based methods but increase the need for comparable data sources.

Although many scientific and development studies have dealt with the detection of individual trees based on ALS data, as far as we know, there is still a relevant demand for an original solution that takes into account the whole three-dimensional structure of the point cloud as well as relations between tree heights, crown diameters, and tree locations. In this context, we developed the xTree tool for the detection of individual trees based on ALS data combining geometric and dendrometric rules (Fig. 1). The first version was introduced into forestry practices in 2017 (Sačkov et al. 2017a). However, the original algorithm still required tree-based training data from field measurements (Sačkov et al. 2016, 2017b, 2019a, 2019b). After several years of refinement, we developed a new version of the xTree tool, containing an enhanced algorithm for simpler, more complex and faster H-based detection of individual trees. Free licenses

Table 1. Case studies focused on elevation model-based detection of individual trees.

Reference	Country	Forest	Samples	Method	Accuracy
Smreček et al. 2017	Slovakia	Mixed	1,286	ZF and CF	67 ±9%
Aubry-Kientz et al. 2019	French Guiana	Broadleaf	1,598	MW and RG, NA and WS	50 ±6%
Sačkov et al. 2019	Slovakia	Mixed	2,003	ZF	58 ±5%
Zaforemska et al. 2019	United Kingdom	Mixed	120	RG, VT, MCWS	87 ±1%
Chen et al. 2020	China	Coniferous	1,453	ZF, WS	27 ±5%
Lisiewicz et al. 2022	Poland	Mixed	1,015	LF, WS with RC	74 ±12%
Sparks et al. 2022	USA	Coniferous	1,928	MW and SW, WS	44 ±1%
Ahmadi et al. 2022	Serbia	Mixed	923	ZF with RC	69 ±5%
Pu et al. 2023	China	Broadleaf	421	FF	91 ±1%
Nemmaoui et al. 2024	Spain	Coniferous	1,355	MCWS, RG	75 ±3%

Note: Samples: number of reference trees; Accuracy: relative proportion of detected trees that match reference trees; ZF: zonal function; CF: cost function; LF: local function; FF: focal function; MW: moving window; NA: neighborhood analysis; RG: region growing; WS: watershed; MCWS: marker-controlled watershed; VT: Voronoi tessellation; RC: result correction; SW: spatial wavelet.

Table 2. Case studies focused on point cloud-based detection of individual trees.

Reference	Country	Forest	Samples	Method	Accuracy
Dalponte et al. 2015	Italy	Mixed	630	KMC	60 ±21%
Amiri et al. 2018	Germany	Coniferous	470	TDS with ASC	66 ±2%
Aubry-Kientz et al. 2019	French Guiana	Broadleaf	1,598	AMSC, MCGC, MCWS	53 ±21%
Zaforemska et al. 2019	United Kingdom	Mixed	120	RG, AMSC	89 ±1%
Sačkov et al. 2019	China	Coniferous	1,453	ZF	53 ±6%
Ma et al. 2020	China	Coniferous	770	RG and KMC	84 ±1%
Torresan et al. 2020	Italy	Mixed	186	HST	46 ±9%
Sparks et al. 2022	USA	Coniferous	1,928	HST	41 ±1%
Pu et al. 2023	China	Broadleaf	421	AMSC, KNC, LSC	98 ±1%
Nemmaoui et al. 2024	Spain	Coniferous	1,355	HST	86 ±1%

Note: Samples: number of reference trees; Accuracy: relative proportion of detected trees that match reference trees; KMC: k-means clustering; TDS: top-down segmentation; ASC: adaptive stopping criterion; AMS: adaptive mean-shift clustering; MCGC: multiclass graph cut; MCWS: marker-controlled watershed; RG: region growing; ZF: zonal function; HST: horizontal spacing threshold; KNC: k-nearest clustering; LSC: layer-stacking clustering.

Table 3. Case studies focused on hybrid-based detection of individual trees.

Reference	Country	Forest	Samples	Data	Method	Accuracy
Dalponte et al. 2015	Italy	Mixed	630	EM and PC	RG, WS	68 ±12%
Sačkov et al. 2016	Italy	Broadleaf	614	PC and API	MW	35 ±9%
Sačkov et al. 2017	Slovakia	Mixed	1332	PC and API	MW	65 ±8%
Sačkov et al. 2017	Slovakia	Mixed	1151	PC and API	MW	70 ±25%
Sačkov et al. 2019	Slovakia	Mixed	2003	PC and API	MW	57 ±1%
Kamińska et al. 2021	Poland	Mixed	1230	PC and AI	RFC	77 ±6%
Sparks et al.2022	USA	Coniferous	1928	EM and PC	WS	43 ±2%
Hui et al. 2022	China	Coniferous	929	EM and PC	MLSAC	84 ±3%
Zhang et al. 2024	China	Mixed	445	EM and AI	LF and RG	84 ±15%
Li et al. 2025	Canada	Mixed	1600	EM and PC	MRS and UC	80 ±1%

Note: Samples: number of reference trees; Accuracy: relative proportion of detected trees that match reference trees; EM: elevation model; PC: point cloud; API: a priori information; AI: aerial image; RG: region growing; WS: watershed; MW: moving window; RFC: random forest classification; MLSAC: multilevel self-adaptive clustering; MRS: mask R-CNN segmentation; UC: U-Net clustering.



Fig. 1. Environments of xTree tool: (a) Original and still supported version requiring tree-based training data from field measurements to calculate dendrometric rules; (b) Enhanced version requiring only a selection of tree species group to calculate dendrometric rules.

are intended for individual non-commercial customers (e.g., researchers, students), and do not apply to the for-profit organizations or companies in any way or form.

In light of the above facts, the primary aim of this article was to present the workflow for H-based detection of individual trees using the xTree tool. For its better understanding and possibility of implementation in other solutions, a detailed description, flowchart, and scheme are provided. The additional aim was to assess the performance of this workflow. For uncovering its time-consuming, completeness, and correctness, a clearly presented scientific results from a case study are provided.

2. Materials and methods

2.1. Model for predicting parameters of dendrometric rules

The detection algorithm of the xTree tool uses a set of dendrometric rules for the verification of the authenticity of detected tree tops. Specifically, these rules relate to the parameters of tree height, crown diameter, and crown length. While the tree height parameter is calculated using a general formula for relative standard deviation, the crown parameters (i.e. diameter and length) are predicted using formulas from original regression models.

These regression models were developed individually for coniferous, broadleaved, and mixed group of tree species. An input dataset consisted of 7,269 measured trees (i.e. 3,397 conifers and 3,872 broadleaf) from various locations in Slovakia (Table 4). The tree species included the Norway spruce (*Picea abies* L. [H.] Karst.), European silver fir (*Abies alba* Mill.), European beech (*Fagus sylvatica* L.), and Sessile oak (*Quercus petraea* Matt.). The tree height and crown length were measured using a hypsometer with a total accuracy of ±1.0 m. The tree diameter was measured using a tree caliper at the millimeter scale. The crown diameter was measured using measuring tape at the centimeter scale. Based on this input dataset, one-parameter nonlinear regression models for the prediction of (1) the ratio of crown diameter to tree height (CDR) and (2) the ratio of crown length to tree height (CLR) were developed. Specifically, the logarithmic function was most suitable for these purposes in terms of strength, significance, and accuracy (Table 5). The strengths of the regression models were assessed using the correlation coefficient. The statistical significances of the regression models were assessed using the t-test at a 0.05 confidence level. The statistical significance of the differences in the regression models was assessed using the Wilcoxon test at the 0.05 confidence level. The accuracies of the regression models were assessed using the relative value of the mean error and the root mean square error.

2.2. Algorithm for detection of individual trees

The workflow for the detection of tree tops and tree crowns using the xTree tool is shown in Fig. 2, and the

Table 4. Input dataset for regression models.

Species Group	T (n)	Ha (m)	Da (cm)	ACDR	ACLR
Coniferous	3,397	22.97 ±8.14	32.52 ±14.01	0.19 ±0.08	0.57 ±0.18
Broadleaved	3,872	22.22 ±8.45	27.12 ±13.71	0.28 ±0.13	0.51 ±0.18
Mixed	7,269	22.57 ±8.31	29.64 ±14.11	0.24 ±0.12	0.53 ±0.18

Note: T: number of trees; Ha: mean height; Da: mean diameter; ACDR: average ratio of crown diameter to tree height with standard deviation; ACLR: average ratio of crown length to tree height with standard deviation.

Table 5. Formulas, accuracy, and significance of regression models.

Species Group	Formulas	R	e%	RMSE%	T test	W test
Coniferous	CDR = –0.1320 ln(h) +0.5975	0.72	0.06	19.45	<0.001	0.125
	CLR = 0.2593 ln(CDR) +1.0087	0.54	0.01	16.87	<0.001	0.163
Broadleaved	CDR = –0.1820 ln(h) +0.8254	0.64	–0.17	24.75	<0.001	0.111
	CLR = 0.2293 ln(CDR) +0.8237	0.57	–0.01	18.60	<0.001	0.158
Mixed	CDR = –0.1620 ln(h) +0.7305	0.63	0.01	27.63	<0.001	0.854
	CLR = 0.1819 ln(CDR) +0.8136	0.49	0.01	20.30	<0.001	0.953

Note: CDR: crown diameter ratio; CLR: crown length ratio; h: tree height in meter; R: correlation coefficient; e%: relative mean error of regression model; RMSE%: relative root mean square error of regression model; T test: p-value of the t-test; W test: p-value of the Wilcoxon test.

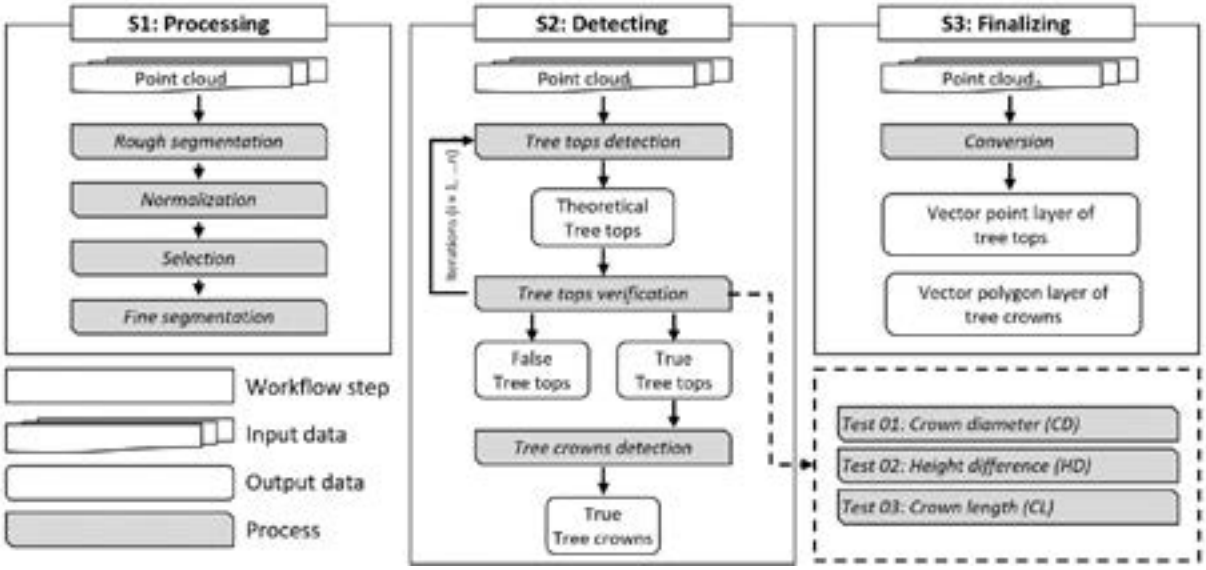


Fig. 2. Scheme of xTree tool algorithm for detection of individual trees.

related steps and process are described in detail in the following sub-sections.

Step S1: Processing

The first step (S1) of the detection algorithm includes four processes (P1.1–1.4) focused on processing the point cloud:

Process P1.1: Rough segmentation

The purpose of this process is to divide the point cloud into regular 3-dimensional rough segments (RSs). These RSs are applied to efficiently use the computer memory and allow for parallel processing of points during the normalization process (i.e. P1.2).

Specifically, the user defines the size of an RS in meters and the process divides the point cloud into the size-related regular RSs. The size of an RS (e.g., default value is 4 × 4) depends on the elevation variability of the ground in the related environment (i.e. higher variability means lower size) and significantly affects the accuracy of point normalization.

Process P1.2: Normalization

The purpose of this process is to provide the aboveground height in meters (i.e. normalized height) for each point within the point cloud.

Specifically, the process firstly calculates the interpolated elevation of the local minima for each RS. The deterministic interpolation of four local minima (i.e. 1 + 3) from eight neighboring RSs (fewer at the edge locations) is used to minimize the local extremes (i.e. negative outliers). The process secondly calculates the normalized height of the points as the difference between the elevation of each point and the interpolated elevation of the local minima within each associated RS. Finally, the process removes points with negative values of normalized height.

Process P1.3: Selection

The purpose of this process is to select relevant points within the point cloud for the second step of the detection algorithm (i.e. S2). This selection is applied to reduce the computation time as well as to place bounds on the minimal (e.g., default value is 3) and maximal (e.g., default value is 50) height of detected trees.

Specifically, the user defines the minimal and maximal height thresholds in meters, and the process removes points below the minimal and above the maximal height.

Process P1.4: Fine segmentation
The purpose of this process is to divide the point cloud into regular 3-dimensional fine segments (FS). These FSs are applied to efficiently use the computer memory and allow for the parallel processing of points during the tree top/crown detection process (i.e. P2.1–2.3).

Specifically, the user defines the size of an FS in meters, and the process divides the point cloud into the size-related regular FSs. The size of an FS (e.g., default value is 2 × 2) depends on the sizes of the tree crown projections in the related environment (i.e. a higher projection means a larger size) and significantly affects the accuracy of tree top/crown detection.

Step S2: Detecting
The second step (S2) of the detection algorithm includes three processes (P2.1–2.3) focused on the detection of tree tops and tree crowns:

Process P2.1: Tree top detection
The purpose of this process is to detect presumed tree tops based on the point cloud delivered by the processing step (i.e. S1).

Specifically, the process iteratively detects the local maxima (i.e. presumed tree tops) using moving-window analysis. This detection is performed in an area covering eight neighboring FSs (fewer at the edge locations). Each of the detected local maxima is referred to as a theoretical tree top (T_{teo}) and then subjected to the tree top verification process (i.e. P2.2). The process of detection is finished if any true tree top is verified.

Process P2.2: Tree top verification
The purpose of this process is to verify the authenticity of the presumed tree tops from the detection process (i.e. P2.1).

Specifically, the user chooses one of three default regression models for the calculation of the test limits (Table 5), and the process verifies the authenticity of T_{teo} through three tests (i.e. T1–3).

The first test (T1) uses a test limit representing tree crown diameter (CD). The process calculates the individual test limit CD for each T_{teo} based on its height and the ratio of its crown diameter to it (eq. [1]). When only one T_{teo} is found in a CD, it is marked as T_{true}. Otherwise, all co-occurring instances of T_{teo} are marked as T_{test} (Fig. 3):

$$CD = HT_{teo} \times CDR \quad [1]$$

where CD is the crown diameter in meters (i.e. the first test limit), HT_{teo} is the height of an individual T_{teo} in meters, and CDR is the ratio of crown diameter to the tree height predicted by the regression model for each individual T_{teo}.

The second test (T2) uses a test limit representing tree height difference (HD). The process first calculates the general HD for the related environment (HDG%). This HDG% is a relative standard deviation of the heights of the 25% highest T_{teo} values (i.e. the third quartile) (eq. [2]). Second, the process detects crown points (CPs) representing the highest points of the FSs located on the connection line between the pairs of T_{test} values. Finally, the process calculates the individual HD for the lower T_{test} in each T_{test} pair based on its height and HDG% value (eq. [3]). When any CP is lower than the individual HD, both T_{test} values are marked as T_{true}. Otherwise, the higher T_{test} is marked as T_{true} and the lower T_{test} is marked as T_{false} (Fig. 4):

$$HDG\% = \frac{SD}{\bar{x}} \times 100 \quad [2]$$

$$SD = \sqrt{\frac{1}{n}\sum_{i=1}^{n} x_i^2 - \bar{x}^2} \qquad \bar{x} = \frac{1}{n}\sum_{i=1}^{n} x_i$$

where HDG% is the general height difference calculated as the relative height variability of the 25% highest T_{teo}

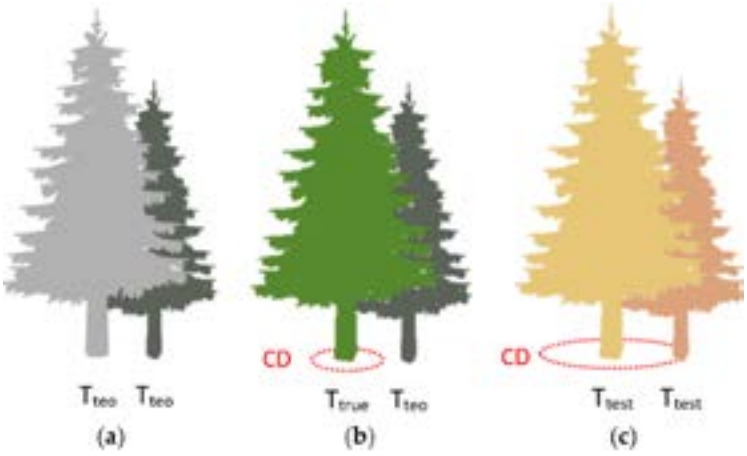


Fig. 3. First test for tree top verification. (a) The process iteratively detects each theoretical tree (T_{teo}) based on local maxima using a moving-window analysis and calculates the individual crown diameter (CD) for each T_{teo} using equation 1. (b) When only one T_{teo} is found in a CD, it is marked as Tt_{rue}; (c) when more than one T_{teo} is found in a CD, they are marked as T_{test}.

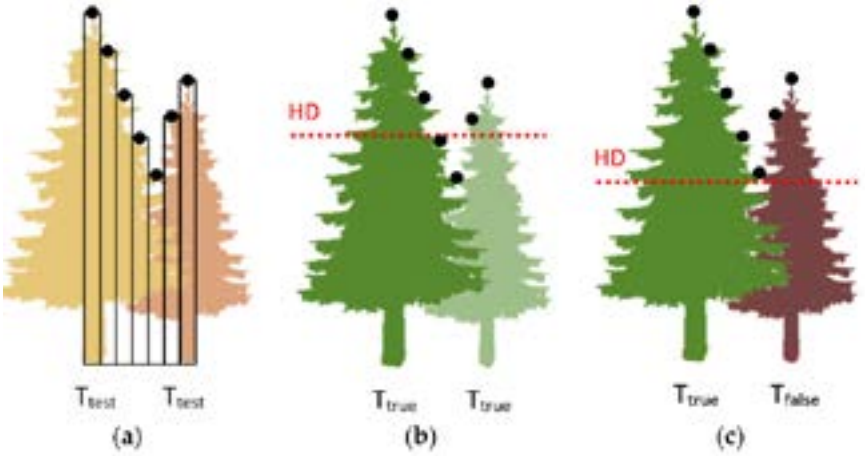


Fig. 4. Second test for tree top verification. (a) The process detects the highest crown points (CPs) located on the connection line between T_{test} pairs and calculates the individual height difference (HD) for the lower T_{test} in each pair using equation 3. (b) When any CP is lower than the individual HD, both T_{test} values are marked as T_{true}; (c) when no CP is lower than the individual HD, the higher T_{test} is marked as T_{true} and the lower T_{test} is marked as T_{false}.

in percentages, SD is the height variability of the 25% highest T_{teo} in meters, $\bar{x}$ is the arithmetic mean of the 25% highest T_{teo} in meters, x is the height of i-th tree in meters, and n is the number of the 25% highest T_{teo};

$$HD = HT_{test} - (HT_{test} \times (HDG\%/100)) \quad [3]$$

where HD is the individual height difference in meters (i.e. the second test limit), HT_{test} is the height of an individual T_{test} in meters, and HDG% is the general height difference, calculated by equation 2, in percentage form.

The third test (T3) uses a test limit representing tree crown length (CL). The process calculates the individual test limits of CD and CL for each T_{true} based on its height and the ratio of the crown length to it (eq. [4]). When any new T_{teo} from the next iteration that is lower than the CL is found in the CD, it is marked as T_{true}. Otherwise, the T_{teo} is marked as T_{false} (Fig. 5):

$$CL = HT_{true} - (HT_{true} \times CLR) \quad [4]$$

where CL is the individual crown length in meters (i.e. the third test limit), HT_{true} is the height of an individual T_{true} in meters, and CLR is the ratio of the crown length to the tree height predicted by the regression model for the individual T_{true}.

Process P2.3: Tree crown detection

The purpose of this process is to detect tree crowns based on the point cloud delivered by the first processing step (i.e. S1).

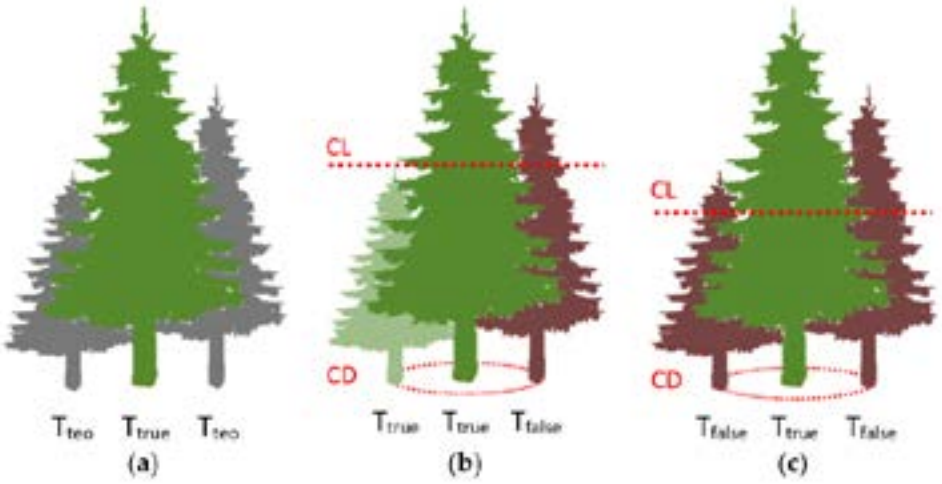


Fig. 5. Third test for tree top verification. (a) The process iteratively detects each new theoretical tree (T_{teo}) based on local maxima using a moving-window analysis and calculates the crown diameter (CD) and crown length (CL) for each T_{true} using equations 1 and 4, respectively. (b) When any new T_{teo} from the next iteration that is lower than the CL is found in the CD, it is marked as T_{true}. (c) When any new T_{teo} from the next iteration that is higher than the CL is found in the CD, it is marked as T_{false}.

Specifically, the process first creates a central crown part (CCP) for each T_{true}. The CCP is a circle with a diameter equal to the size of the FS. Second, the process repeatedly creates peripheral crown parts (PCPs) to the nearest CCP. The PCPs are stripes around the CCP with edges equal to half of the size of the FS. This process is finished when the new CCPs meet any point already assigned to another CCP or until they reach the test limits of the CD and CL. Third, the process (1) assigns the CCP and PCPs to a single T_{true}, (2) creates a tree crown based on the shape of the border PCPs, (3) smooths the tree crown based on the Bezier interpolation, and (4) creates the true tree crown. Finally, the process assigns the points from the cloud located within the area of the true crown to this single T_{true} (Fig. 6).

Step S3: Finalizing

The third step (S3) of the detection algorithm includes one process (P3.1) focused on the conversion of tree tops and tree crowns:

Process P3.1: Conversion

The purpose of this process is to convert the tree tops and tree crowns detected in the second step of the detection algorithm (i.e. S2) into vector layers.

Specifically, the process converts the true tree tops to point layers in the ESRI Shapefile format and the true tree crowns to polygon layers in the ESRI Shapefile format (Fig. 7). These layers use the original coordinate system of the point cloud, and the attribute table includes (1) unique identifiers for the tree tops and tree crowns, (2) connecting identifiers between pairs of tree tops and tree crowns, (3) values of tree heights in meters, and (4) values of tree crown projections in square meters.

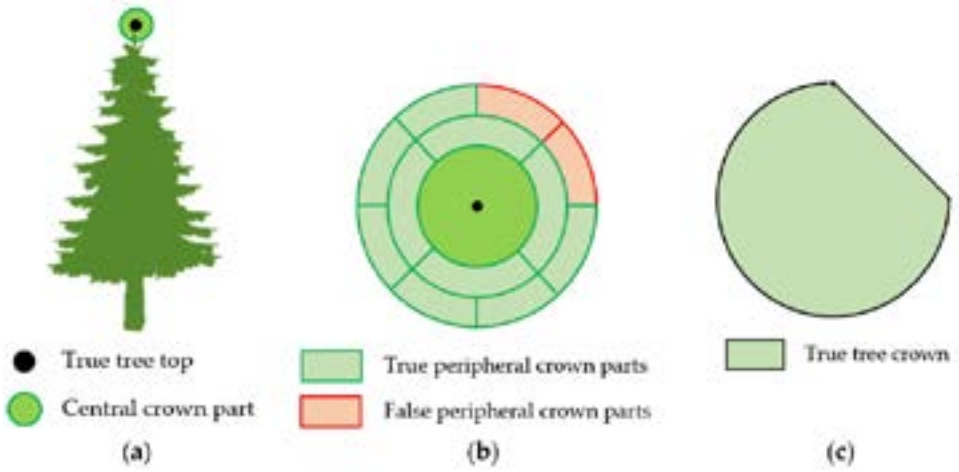


Fig. 6. Process for tree crown detection. (a) The process creates a central crown part (CCP) for each T_{true} as a circle with a diameter equal to the size of the FS. (b) The process repeatedly creates peripheral crown parts (PCPs) to the nearest CCP as stripes around it, with edges equal to half of the size of the FS. This process is finished when the new CCPs meet any point already assigned to another CCP or until they reach the test limits of the CD and CL. (c) The process assigns the CCP and PCPs to a single T_{true}, creates a tree crown based on the shape of the border PCPs, smooths the tree crown using the Bezier interpolation, and creates the true tree crown.

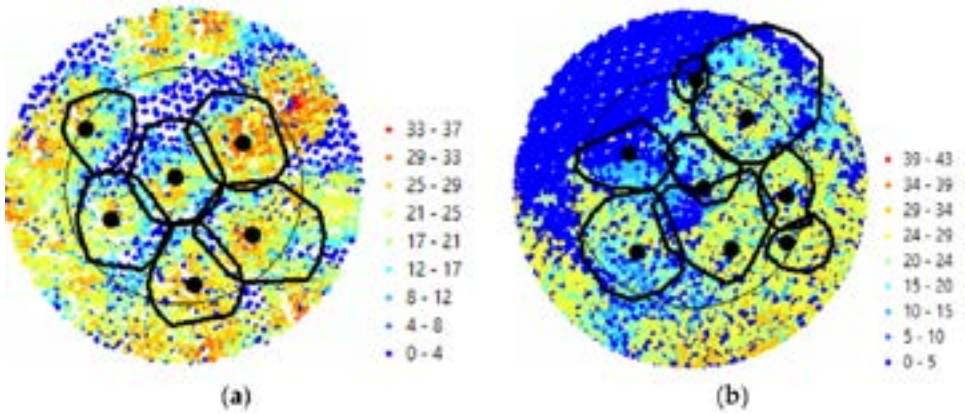


Fig. 7. Example of detection results: (a) Coniferous trees; (b) Broadleaved trees. Note: Thin black line: sample plot; bold black lines: position and shape of tree tops; black points: position of tree tops.

2.3. Performance analysis of detection algorithm

Study area

The performance analysis was conducted within two territories in Slovakia (Fig. 8). The northern territory (49°29´N, 18°52´E) is located at an altitude of 511–1,110 m a.s.l., and its dominant tree species include the Norway spruce (*Picea abies*), European silver fir (*Abies alba*), and European red pine (*Pinus sylvestris* L.). The central territory (48°32´N, 19°23´E) is located at an altitude of 331–932 m a.s.l., and its dominant tree species include the European beech (*Fagus sylvatica*), Sessile oak (*Quercus petraea*), and Norway spruce (*Picea abies*).

Ground reference data

A total of 90 circular sample plots with radii of 10 m each were located in the northern and central territories of the study area and subsequently divided into 9 strata (i.e. 10 plots per stratum). The main criteria for stratification were tree species composition and mean diameter. Specifically, strata dominated by (1) coniferous trees (C≥95%), (2) broadleaved trees (B≥95%), and (3) mixed coniferous and broadleaved trees (M = C/B ≈ 50%/50%) were created. Each stratum was further divided into three development stages defined by the mean diameter (C1/B1/M1 = 6–19 cm, C2/B2/M2 = 20–35 cm, and C3/B3/M3 > 36 cm). An overview of the ground reference data for each stratum is presented in Table 6–8.

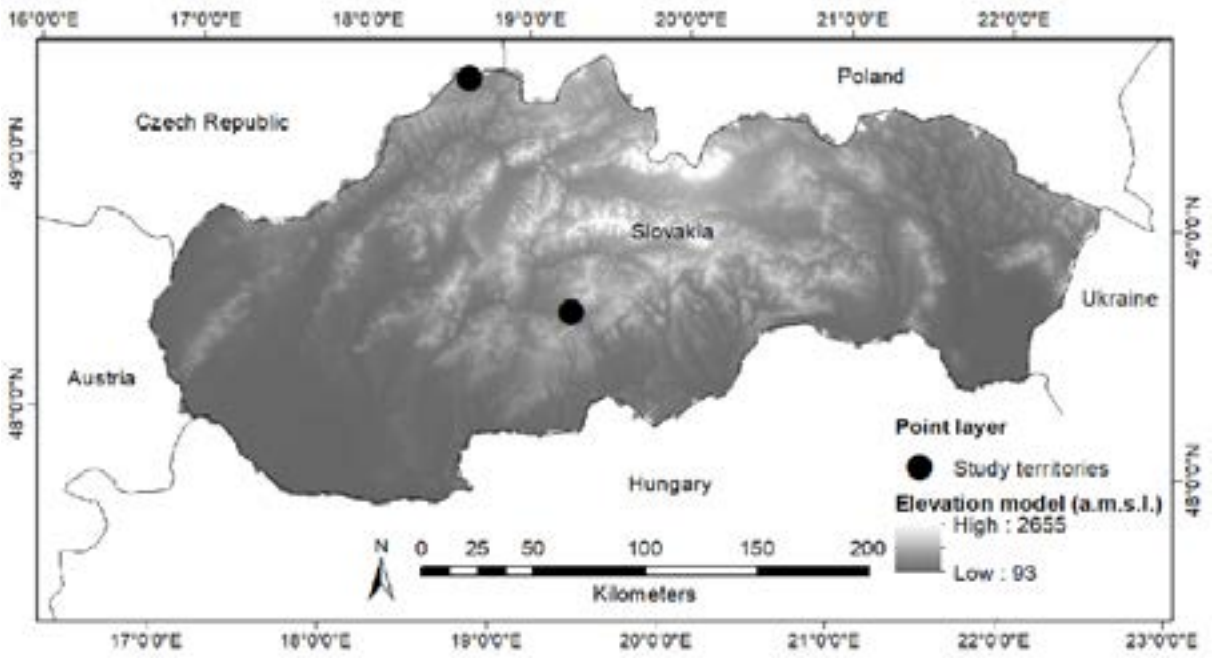


Fig. 8. Study area containing the central and north territories.

Table 6. Ground reference data for coniferous stratum.

Stratum	SP (n)	A (ha)	T (n)	Ha (m)	Da (cm)	V (m³)	VA (m³/ha)	TA (n/ha)
C1	10	0.31	384	11.72	13.20	40.63	129.99	1,232
C2	10	0.31	211	22.07	27.57	156.71	501.36	675
C3	10	0.31	108	31.19	40.52	191.55	612.82	346
Total	30	0.94	703	—	—	388.89	—	—
Average	10	0.31	234	21.66	27.10	129.63	414.72	751

Note: SP: sample plot; A: area; T: number of trees; Ha: mean height; Da: mean diameter; V: total volume; VA: hectare volume; TA: number of trees in hectare.

Table 7. Ground reference data for broadleaved stratum.

Stratum	SP (n)	A (ha)	T (n)	Ha (m)	Da (cm)	V (m³)	VA (m³/ha)	TA (n/ha)
B1	10	0.31	486	13.75	14.17	60.80	194.52	1,555
B2	10	0.31	185	23.47	27.13	157.22	502.99	592
B3	10	0.31	68	29.61	41.91	144.27	461.56	218
Total	30	0.94	739	—	—	362.29	—	—
Average	10	0.31	246	22.28	27.74	120.76	386.36	788

Note: SP: sample plot; A: area; T: number of trees; Ha: mean height; Da: mean diameter; V: total volume; VA: hectare volume; TA: number of trees in hectare.

Table 8. Ground reference data for mixed stratum.

Stratum	SP (n)	A (ha)	T (n)	Ha (m)	Da (cm)	V (m^3)	VA (m^3/ha)	TA (n/ha)
M1	10	0.31	376	14.03	16.91	62.38	199.57	1,203
M2	10	0.31	193	20.98	25.64	140.10	448.22	617
M3	10	0.31	108	30.53	39.99	192.44	615.67	345
Total	30	0.94	677	—	—	394.92	—	—
Average	10	0.31	226	21.85	27.52	131.64	421.15	772

Note: SP: sample plot; A: area; T: number of trees; Ha: mean height; Da: mean diameter; V: total volume; VA: hectare volume; TA: number of trees in hectare.

The ground reference data from the northern territory were obtained during the leaf-on season in 2022 within 44 circular sample plots (1.38 ha). The ground reference data from the central territory were obtained during the leaf-on season in 2021 within 46 circular sample plots (1.44 ha). Specifically, the position of the plot center was located using the GNSS, with a positional error from 1.44 to 6.25 m. A total of 2,119 trees were measured in terms of species, height, and diameter. Tree height was measured using the Vertex IV hypsometer (Haglöf Inc.), with a total accuracy of ±1.0 m. Measurement of tree diameter was performed with a tree caliper at the millimeter scale. The tree volume was calculated based on two-parameter allometric model (i.e. height and diameter), with a total accuracy of 10% (Petráš & Pajtík 1991).

Airborne laser scanning data

ALS data acquisitions were performed in September 2022 for the northern territory and in June 2021 for the central territory using a Leica ALS 70 CM scanner (Leica Geosystems AG). Both territories were scanned from an average altitude of 1,300 m with a 43° field of view and a 281.8 kHz laser pulse repetition rate. An average overlap between 700 m wide strips was set to 30%. The resulting vertical standard error was 0.05 m, and the average density of the point cloud reached 18 ±6 point/m^2. In further processing, positive and negative outliers (i.e. points with disproportionately higher or lower altitudes than the altitudes of neighboring points) were removed.

Evaluation of detection performance

The first part of evaluation was focused on the time consumption of detection. This was evaluated based on a chronometry of all detection processes (i.e. P1–3). Related detection was performed for overall sample size using high-performance workstation (Table 9) with default settings (i.e. rough segment is 4 m, fine segment is 2 m, minimal height is 3 m, and maximal heigh is 50 m).

Table 9. Technical specifications for high-performance workstation.

Attribute	Specifications
Processor (frequency, cache, cores)	2.3/3.9 GHz, 22 MB, 16
Memory (capacity, speed)	128 GB RAM, 2,666 MHz
Graphic card (memory, speed, cores)	16 GB, 1620 MHZ, 48
Internal storage (capacity and type)	1 TB SSD, 4 TB HDD, 4 TB HDD
System	Microsoft Windows 10 Pro

The second part of evaluation was focused on the accuracy of detection. This was evaluated based on a pairwise comparison of the reference trees and detected trees. The matching of the reference and detected trees was carried out manually by geospatial observation of the positions (i.e. closest distance between trees) and heights (i.e. smallest height difference between trees) of the related trees. In order to minimize the subjective bias, this matching process involved three independent observations. Moreover, there were two levels of evaluation:

- The first level of evaluation assessed the total detection performance for individual strata (i.e. C, B, M) as well as for overall sample size regardless of stratification (i.e. C + B + M). Specifically, the correctness of detection was calculated as the ratio of the number of detected trees that were successfully linked to reference trees from the total number of detected trees. The completeness of detection was calculated as (1) the ratio of the number of reference trees, from the total thereof, that were associated with detected trees (i.e. number completeness) and (2) the ratio of the volume of reference trees, from the total volume thereof, that were associated with detected trees (i.e. volume completeness). The volume of detected trees was calculated based on a combination of allometric models with a total accuracy of 19% (Sačkov et al. 2019a, 2019b).
- The second level of evaluation assessed the interval detection performance for individual strata. Specifically, the interval detection performance was calculated as the number of detected trees that were successfully linked to reference trees within a specific interval of tree height. This interval was set to 3 m and covered the whole range of tree heights.

3. Results

3.1. Time performance of enhanced algorithm

Detection of 1,719 individual trees from 90 sample plots with an area of 2.8 ha using the xTree tool took 696 seconds (i.e. 248 s/ha or 0.4 s/tree). The individual processes shared this time, with ratios of 22.5% within the processing step (i.e. S1), 77% within the detecting step (i.e. S2), and 0.5% within the finalizing step (i.e. S3).

3.2. Total detection performance of enhanced algorithm

The results of the performance analysis are summarized in Table 10. The detection algorithm achieved overall correctness within an interval of 75–95%. The overall completeness based on tree numbers was within an interval of 51–87%, and the overall completeness based on tree volume was within an interval of 67–89%. Generally, the performance increased with the increasing proportion of coniferous trees and value of tree diameters.

Table 10. Correctness and completeness of detection algorithm.

Stratum	Correctness (%)	Number Completeness (%)	Volume Completeness (%)
Coniferous	89 ±2	71 ±6	79 ±4
C1	86 ±5	67 ±10	75 ±7
C2	93 ±3	72 ±8	77 ±5
C3	92 ±4	81 ±10	84 ±9
Broadleaved	84 ±4	66 ±8	76 ±5
B1	82 ±7	64 ±10	70 ±7
B2	86 ±5	68 ±16	78 ±11
B3	87 ±8	76 ±10	81 ±9
Mixed	82 ±4	70 ±6	79 ±4
M1	80 ±6	65 ±8	72 ±6
M2	82 ±7	72 ±9	79 ±6
M3	85 ±8	81 ±11	85 ±9
Overall	85 ±2	69 ±4	78 ±2

Note: Correctness and completeness with standard error at the 95% confidence interval.

Visual examples of the detection results are presented in Fig. 9–11. Specifically, random examples of one sample plot from each stratum include 191 reference trees and 120 detected trees, containing 2 false-positive trees in the coniferous stratum and 4 false-positive trees in the broadleaved stratum.

3.3. Interval detection performance of enhanced algorithm

From the interval frequencies of the reference and correctly detected trees, we were able to summarize the vertical distribution of 205 omitted and 62 committed trees in the conifer stratum (Fig. 12a–d), 250 omitted and 94 committed trees in the broadleaved stratum (Fig. 13a–d),

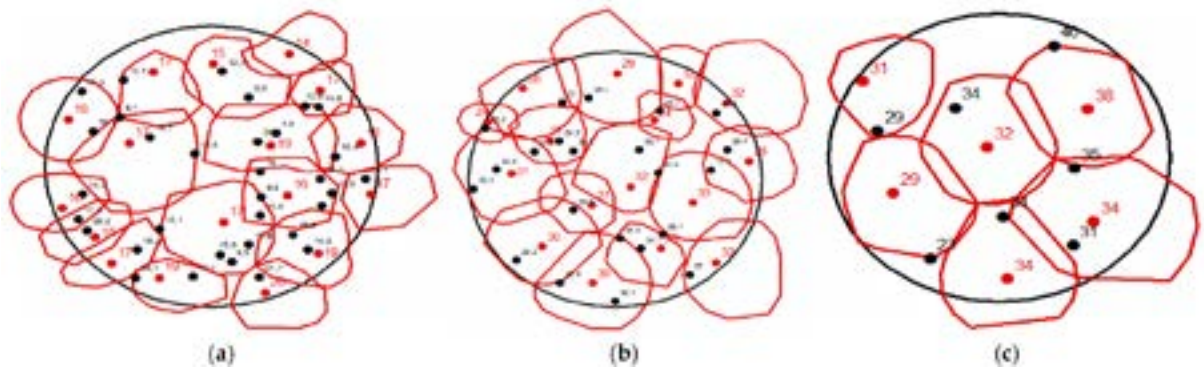


Fig. 9. Examples of detection results: (a) Stratum C1; (b) Stratum C2; and (c) Stratum C3. Note: black line: sample plot; black point and number: position and height of each reference tree top; red point and number: position and height of each detected tree top; red line: position and shape of each detected tree crown.

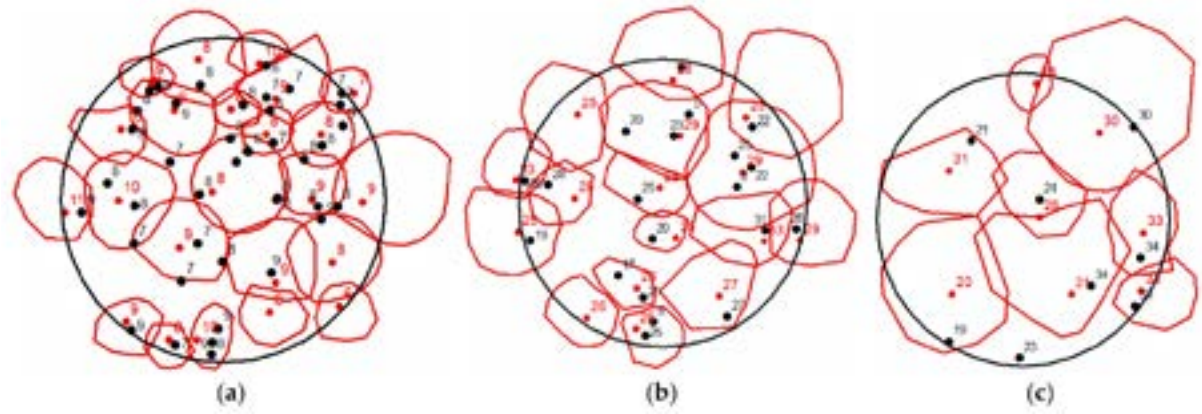


Fig. 10. Examples of detection results: (a) Stratum B1; (b) Stratum B2; (c) Stratum B3. Note: black line: sample plot; black point and number: position and height of each reference tree top; red point and number: position and height of each detected tree top; red line: position and shape of each detected tree crown.

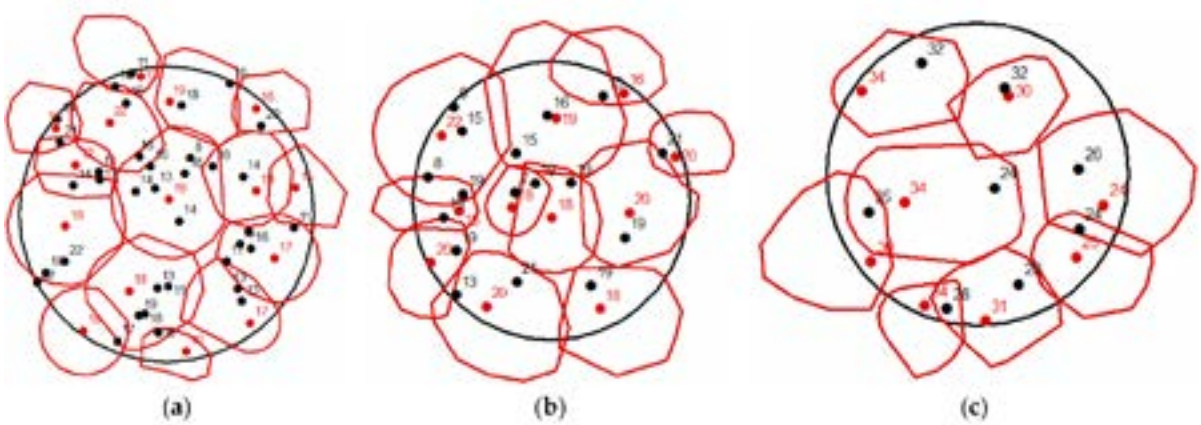


Fig. 11. Examples of detection results: (a) stratum M1; (b) stratum M2; (c) stratum M3. Note: black line: sample plot; black point and number: position and height of each reference tree top; red point and number: position and height of each detected tree tops; red line: position and shape of each detected tree crowns.

and 206 omitted and 105 committed trees in the mixed stratum (Fig. 14a–d). Generally, performance extremely increased with increasing tree heights.

4. Discussion

4.1. Relevance of detection algorithm

The tree-based variables (e.g., height, diameter, volume, position, species, condition) are integral part of various quantitative as well as qualitative forest inventories (e.g., forest management inventory, national forest inventory, forest health monitoring) that play key roles in sustainable forest management (Bettinger et al. 2016). In particular, ALS has recently received much attention as an innovative technology capable of improving the efficiency of traditional field measurement of these tree-based variables (Zhen et al. 2016).

Given these relationships (i.e. forestry requirements and ALS potential), we have developed the xTree tool, which is provided for non-commercial purposes as a free desktop application.

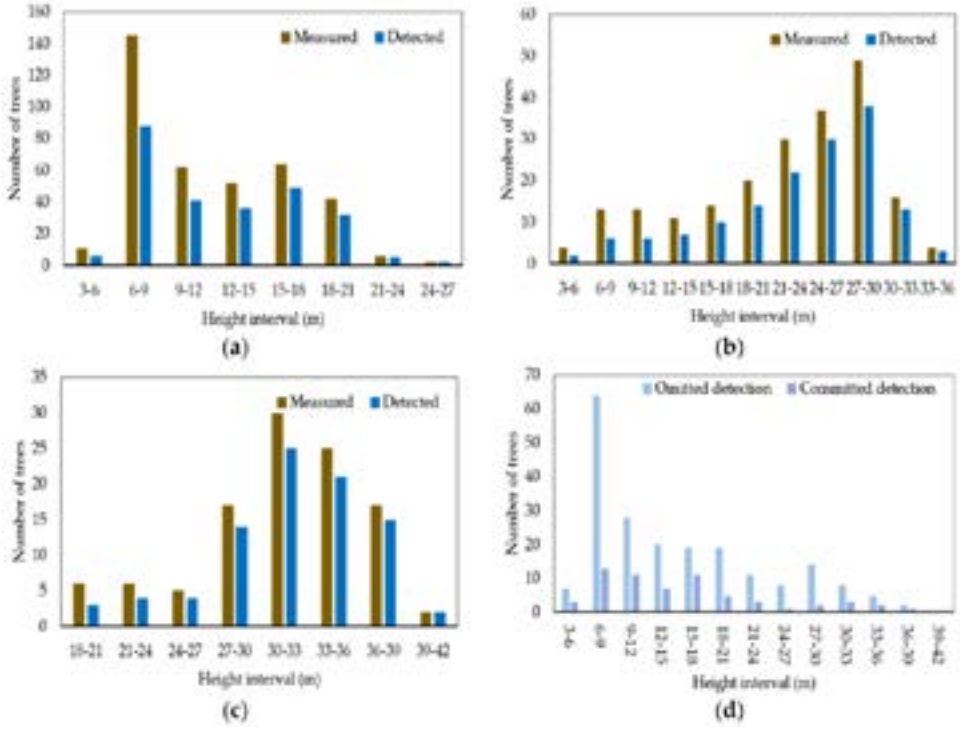


Fig. 12. Interval performance of detection algorithm: (a) numbers of reference and correctly detected trees for stratum C1; (b) numbers of reference and correctly detected trees for stratum C2; (c) numbers of reference and correctly detected trees for stratum C3; and (d) numbers of omitted and committed trees for the conifer stratum.

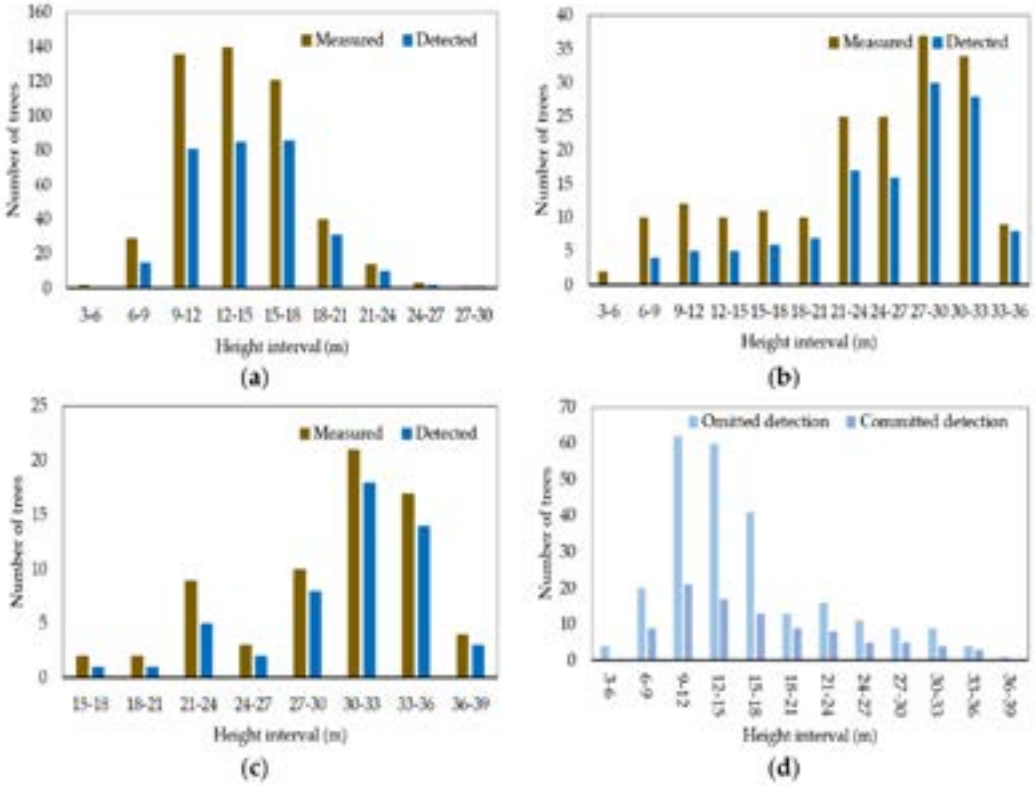


Fig. 13. Interval performance of detection algorithm: (a) numbers of reference and correctly detected trees for stratum B1; (b) numbers of reference and correctly detected trees for stratum B2; (c) numbers of reference and correctly detected trees for stratum B3; and (d) numbers of omitted and committed trees for the broadleaved stratum.

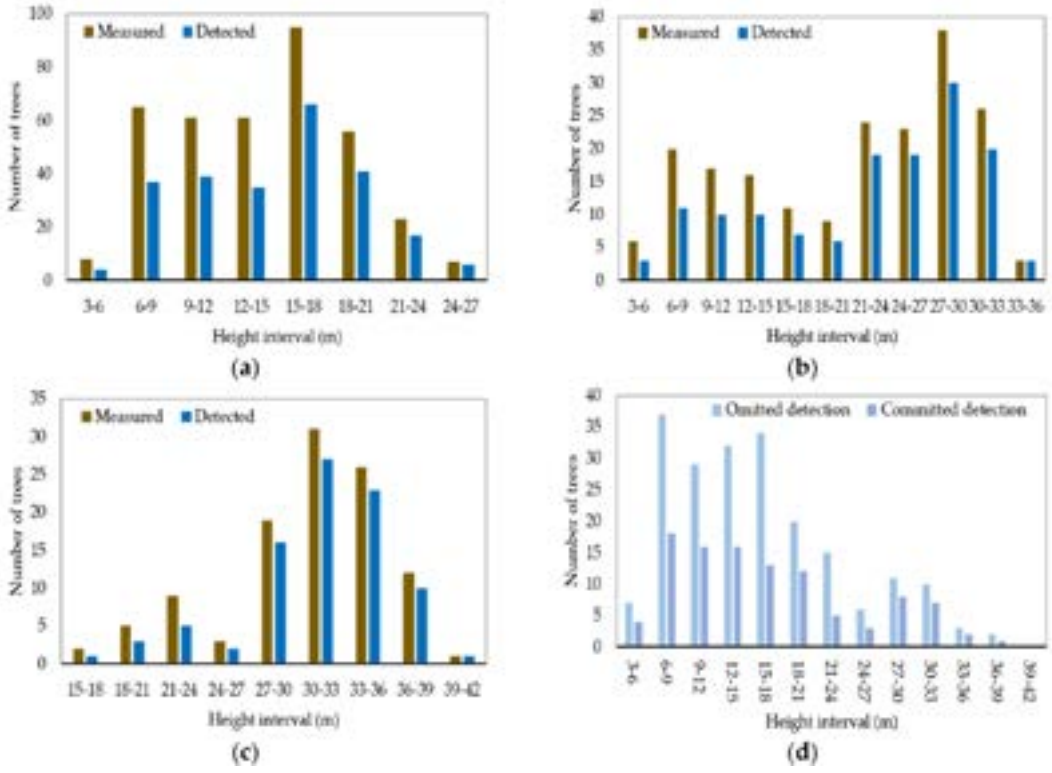


Fig. 14. Interval performance of detection algorithm: (a) numbers of reference and correctly detected trees for stratum M1; (b) numbers of reference and correctly detected trees for stratum M2; (c) numbers of reference and correctly detected trees for stratum M3; and (d) numbers of omitted and committed trees for the mixed stratum.

4.2. Pros and Cons of detection algorithm

In contrast to other EM/PC/H-based solutions for the detection of individual trees, the enhanced algorithm of current version of the xTree tool provides several unique features:

- The xTree tool is user-friendly because (1) the interface includes generally used elements of desktop application (e.g., windows, icons, buttons), (2) the outputs include the generally used format of vector layers (i.e. SHP), and (3) the workflow includes original models for the automatic adjustment of related geometric and dendrometric rules (i.e. ratio of crown diameter to tree height and ratio of crown length to tree height). Unlike other tool-based solutions (e.g., McGaughey 2024), there is no need to encode script, convert data, or measure training data in the field. However, original models from xTree tool are specifically oriented to the conditions of Central European forests and are not globally generalizable. In these non-European cases, it is necessary to use a version of tool that reqires local training tree-based data (Fig. 1a).
- The xTree tool is comprehensive because its workflow considers the entire three-dimensional structure of the original point cloud, as well as the relations between the variables of detected trees. Tree tops and tree crowns are iteratively detected based on the heights of segmented ALS points and verified based on limits representing supposed (1) crown diameters, (2) differences between tree heights, and (3) crown lengths. Moreover, these limits are unique for each detected tree. Although a few other H-based methods use some tree-based variables, such as minimal tree height or average/maximal crown diameter (e.g., Ayrey et al. 2017), most from other methods use a priori information from elevation models, aerial images, or additional field measurement (e.g., Ene et al. 2012; Li et al. 2012; Sparks et al. 2022). On the other hand, complexity of the xTree tool increases the requirements for specific hardware and detection time.
- The xTree tool is efficient because its workflow (1) uses parallel processing to handle separate parts of individual tasks using two or more processors, (2) divides the original point cloud into regular three-dimensional segments at two levels of resolution (i.e. rough segments for normalization and fine segments for detection), and (3) reduces the number of ALS points based on the minimal and maximal height thresholds. However, efficiency of the xTree tool is extremely affected by hardware used and total number of ALS points processed.

4.3. Applicability of detection algorithm

The detection of individual trees using the enhanced algorithm of the xTree tool was verified through a case study. The study area covered 2.8 ha of forests in Slovakia. The ALS data reached an average density of 18 ±6 points/m^2. The ground reference data included 90 sample plots with 703 trees in the coniferous stratum, 739 trees in the broadleaved stratum, and 677 trees in the mixed stratum. Moreover, these strata were divided into three development stages (Tables 6–8).

The evaluation of time performance showed that the detection algorithm consumed 248 seconds per hectare, or 0.4 of a second per tree. Tree top/crown detection and verification (i.e. the second step) were the most time-consuming processes, with a ratio of up to 77%. These findings are very important for time management of applications, especially for larger forest units. However, the associated time complexity depends extremely on the architecture of the workstation, point cloud density, and algorithm setting (i.e. sizes of RS and FS).

The evaluation of the accuracy performance showed that average completeness (Table 10), also called recall and representing the ratio of correctly detected trees to all reference trees, was, in the case of tree number, 71 ±6% in the coniferous stratum, 66 ±8% in the broadleaved stratum, and 70 ±6% in the mixed stratum (i.e. 69 ±4% for all strata). In the case of tree volume, it was 79 ±4% in the coniferous stratum, 76 ±5% in the broadleaved stratum, and 79 ±4% in the mixed stratum (i.e. 78 ±2% for all strata). Although the coniferous stratum achieved the highest accuracy here, the tree species composition did not have an extraordinary impact on detection results. On the other hand, the accuracy values between development stages (Table 10) and between height intervals (Fig. 12–14) were considerable different. They increased with increasing tree dimensions (i.e. tree height and diameter) and decreasing tree numbers (i.e. tree density). Specifically, the average differences between the accuracy of the first and last development stage (i.e. C1/B1/M1 vs. C3/B3/M3) and between the accuracy of the first and last height interval (i.e. 3–6 m vs. 39–42 m) were 14 ±2% and 42 ±11%, respectively. This is because the high density of trees typical in the young development stages of forests decreases the clarity of tree tops and crowns. Moreover, a dense tree canopy, regardless of development stages, will reduce the density of the point clouds within the understory. For example, our point cloud included only 6% of the points in the space below the median tree height of the individual development stages. However, this space included up to 43% of these trees. The associated omission error therefore mainly concerns understory trees (i.e. intermediate and suppressed), which is, however, the objective challenge of most of detection algorithms. Specifically, the detection ratios of suppressed trees are usually in the range of 5–21% (Solberg et al. 2006; Ferraz et al. 2012; Dun-

canson et al. 2014; Lu et al. 2014; Sačkov et al. 2019b). In this context, many other studies suggest using ALS data from leaf-off season or a specific algorithm to refine detection results (Lahivaara et al. 2014; Melville et al. 2015; Kansanen et al. 2016).

The evaluation of accuracy performance further showed that the average correctness (Table 10), also called precision and representing the ratio of correctly detected trees to all detected trees, was 89 ±2% in the coniferous stratum, 84 ±4% in the broadleaved stratum, and 82 ±4% in the mixed stratum (i.e. 85 ±2% for all strata). In this case, tree species composition, development stage, and forest structure did not have extraordinary impacts on the detection results. Specifically, the related differences achieved an interval of only 5–6% (Table 10). The main reason was the relatively small level of commission error (i.e. 12 ±3%). Thus, the tree top verification process of the enhanced algorithm (i.e. P2.2) was relatively successful in suppressing false tree tops, such as protruding branches, multiple terminals, and other morphological patterns of tree crowns. The key feature here was the model for the prediction of dendrometric rules, which iteratively provided verification limits representing the supposed crown diameter, difference between tree heights, and crown length for each detected tree.

An overview of the most relevant studies focusing on the detection of individual trees based on ALS data over the last decade confirmed our results. In those studies, the average completeness values based on tree number using H-based methods (Table 3) were 70 ±21% in coniferous forests, 69 ±21% in broadleaved forests, and 71 ±13% in mixed forests (i.e. 70 ±17% for all forests). Thus, the completeness of the xTree algorithm was on a similar level to other studies. On other hand, the detection algorithm of the xTree tool did exceed the correctness reported by the other studies (i.e. 80 ±16% for all forests) (e.g., Sačkov et al. 2019b; Sparks et al. 2022; Pu et al. 2023). Thus, it was 5% more accurate (Table 10). These and other studies define the detection method (i.e. EM, PC, and H) and quality of the point cloud (i.e. point density) as the most important factor affecting the performance of detection results. However, even more relevant to our results, the next-most important factor was the defined vertical and horizontal structure of the forest (Kaartinen et al. 2012; Vauhkonen et al. 2014; Mongus 2015).

5. Conclusions

This article presents the workflow and applicability of the authors' geoprocessing tool, xTree, which was designed for the detection of individual trees based on a combination of ALS data and a priori information (i.e. geometric and dendrometric rules).

The following are the key findings:

- The xTree tool represents a non-commercial desktop application that allows for the detection of tree tops and tree crowns. The associated algorithm requires only the ALS point cloud as an input dataset and provides vector layers in the ESRI Shapefile format as output datasets. It includes original models for automatic adjustment of related geometric and dendrometric rules (i.e. a priori information). There is no need to encode script, convert data, or measure training data in the field.
- The case study presented herein showed that the detection of individual trees using the xTree tool could take 0.4 of a second per tree and achieved overall correctness of 85 ±2%. The overall completeness based on tree number was 69 ±4%, and the overall completeness based on tree volume was 78 ±2% (Table 10).
- Future improvement of the xTree tool could include (1) simplifying the most time-consuming process of the algorithm (i.e. P2.1 and P2.2) and (2) developing a new algorithm to refine the detection results (e.g., a model for the virtualization of understory trees). Additionally, future scientific case studies could uncover sensitivity and uncertainty of individual process (e.g., normalization, tree top detection and verification, tree crown detection) related to the different tool setting (e.g., size of RS and FS) and forest environment (e.g., sparse and dense forest, one-layered and multi-layered forest).

Acknowledgements

This article is based on results from the project "Development of advanced geospatial technologies for multiscale monitoring of forest ecosystems (APVV-19-0257)" and "High-tech national forest inventory based on mobile laser scanning: from research to realization (APVV-24-0064)" supported by the Slovak Research and Development Agency.

References

Ahmadi, S. A, Ghorbanian, A., Golparvar, F., Mohammadzadeh, A., Jamali, S., 2022: Individual tree detection from unmanned aerial vehicle (UAV) derived point cloud data in a mixed broadleaf forest using hierarchical graph approach. European Journal of Remote Sensing, 55:520–39.

Amiri, N., Polewski, P., Heurich, M., Krzystek, P., Skidmore, A. K., 2018: Adaptive stopping criterion for top-down segmentation of ALS point clouds in

temperate coniferous forests. ISPRS Journal of Photogrammetry and Remote Sensing, 141:265–74.

Aubry-Kientz, M., Dutrieux, R., Ferraz, A., Saatchi, S., Hamraz, H., Williams, J. et al., 2019: A Comparative Assessment of the Performance of Individual Tree Crowns Delineation Algorithms from ALS Data in Tropical Forests. Remote Sensing, 11:1086.

Ayrey, E., Fraver, S., Kershaw, J. J., Kenefic, L. S., Hayes, D., Weiskittel, A. R. et al., 2017: Layer Stacking: A Novel Algorithm for Individual Forest Tree Segmentation from LiDAR Point Clouds. Canadian Journal of Remote Sensing, 43:16–27.

Bettinger, P., Boston, K., Siry, J. P., Grebner, D. L., 2016: Forest Management and Planning. New York, USA, Academic Press, 363 p.

Dalponte, M., Reyes, F., Kandare, K., Gianelle, D., 2015: Delineation of Individual Tree Crowns from ALS and Hyperspectral data: a comparison among four methods. European Journal of Remote Sensing, 48:365–82.

Duncanson, L. I., Cook, B. D., Hurtt, G. C., Dubayah, R. O., 2014: An efficient, multi-layered crown delineation algorithm for mapping individual tree structure across multiple ecosystems. Remote Sensing and Environment, 154:378–86.

Ene, L., Næsset, E., Gobakken, T., 2012: Single tree detection in heterogeneous boreal forests using airborne laser scanning and area-based stem number estimates. Internatoional Journal of Remote Sensing, 33:5171–5193.

Eysn, L., Hollaus, M., Lindberg, E., Berger, F., Monnet, J. M., Dalponte, M. et al., 2015: A Benchmark of Lidar-Based Single Tree Detection Methods Using Heterogeneous Forest Data from the Alpine Space. Forests, 6:1721–1747.

Ferraz, A., Bretar, F., Jacquemoud, S., Gonçalves, G., Pereira, L., Tomé, M. et al., 2012: 3-D mapping of a multi-layered Mediterranean forest using ALS data. Remote Sensing and Environment, 121:210–223.

Hui, Z., Cheng, P., Yang, B., Zhou, G., 2022: Multi-level self-adaptive individual tree detection for coniferous forest using airborne LiDAR. International Jornal of Applied Earth Observation and Geoinformation, 114:103028.

Chen, W., Xiang, H., Moriya, K., 2020: Individual Tree Position Extraction and Structural Parameter Retrieval Based on Airborne LiDAR Data: Performance Evaluation and Comparison of Four Algorithms. Remote Sensing, 12:571.

Kaartinen, H., Hyyppä, J., Yu, X., Vastaranta, M., Hyyppä, H., Kukko, A. et al., 2012: An International Comparison of Individual Tree Detection and Extraction Using Airborne Laser Scanning. Remote Sensing, 4:950–974.

Kamińska, A., Lisiewicz, M., Stereńczak, K., 2021: Single Tree Classification Using Multi-Temporal ALS Data and CIR Imagery in Mixed Old-Growth Forest in Poland. Remote Sensing, 13:5101.

Kansanen, K., Vauhkonen, J., Lahivaara, T., Mehtatalo, L., 2016: Stand density estimators based on individual tree detection and stochastic geometry. Canadian Journal of Forest Research, 46:1359–1366.

Lahivaara, T., Seppanen, A., Kaipio, J. P., Vauhkonen, J., Korhonen, L., Tokola, T. et al., 2014: Bayesian approach to tree detection based on airborne laser scanning data. IEEE Transaction on Geoscience and Remote Sensing, 52:2690–2699.

Li, Q., Hu, B., Shang, J., Remmel, T. K., 2025: Two-Stage Deep Learning Framework for Individual Tree Crown Detection and Delineation in Mixed-Wood Forests Using High-Resolution Light Detection and Ranging Data. Remote Sensing, 17:1578.

Li, W., Guo, Q., Jakubowski, M. K., Kelly, M., 2012: A New Method for Segmenting Individual Trees from the Lidar Point Cloud. Photogrammetric Enginneering and Remote Sensing, 78:75–84.

Lisiewicz, M., Kamińska, A., Kraszewski, B., Stereńczak, K., 2022: Correcting the Results of CHM-Based Individual Tree Detection Algorithms to Improve Their Accuracy and Reliability, Remote Sensing, 14:1822.

Lu, X., Guo, Q., Li, W., Flanagan, J. A., 2014: Bottom-up approach to segment individual deciduous trees using leaf-off lidar point cloud data. ISPRS Journal of Photogrammtry and Remote Sensing, 94:1–12.

Ma, Z., Pang, Y., Wang, D., Liang, X., Chen, B., Lu, H. et al., 2020: Individual Tree Crown Segmentation of a Larch Plantation Using Airborne Laser Scanning Data Based on Region Growing and Canopy Morphology Features. Remote Sensing, 12:1078.

Melville, G., Stone, C., Turner, R., 2015: Application of LiDAR data to maximise the efficiency of inventory plots in softwood plantations. New Zeland Journal of Forestry Science, 45:9.

Mongus, D., Žalik, B., 2015: An efficient approach to 3D single tree-crown delineation in LiDAR data. ISPRS J Photogrammetry and Remote Sensing, 108:219–233.

Nemmaoui, A., Aguilar, F. J., Aguilar, M. A., 2024: Benchmarking of Individual Tree Segmentation Methods in Mediterranean Forest Based on Point Clouds from Unmanned Aerial Vehicle Imagery and Low-Density Airborne Laser Scanning. Remote Sensing, 16:3974.

Petráš, R., Pajtík, J., 1991: Sústava česko-slovenských objemových tabuliek drevín. Lesnícky časopis, 37:49–56. (In Slovak).

Pu, Y., Xu, D., Wang, H., Li, X., Xu, X., 2023: A New Strategy for Individual Tree Detection and Segmentation from Leaf-on and Leaf-off UAV-LiDAR Point Clouds Based on Automatic Detection of Seed Points. Remote Sensing, 15:1619.

Sačkov, I., Santopuoli, G., Bucha, T., Lasserre, B., Marchetti, M., 2016: Forest Inventory Attribute Prediction Using Lightweight Aerial Scanner Data in a Selected Type of Multilayered Deciduous Forest. Forests, 7:307.

Sačkov, I., Hlásny, T., Bucha, T., Juriš, M., 2017a: Integration of tree allometry rules to treetops detection and tree crowns delineation using airborne lidar data. IForest – Biogeosciences and Forestry, 10:459.

Sačkov, I., Sedliak, M., Kulla, L., Bucha, T., 2017b: Inventory of Close-to-Nature Forests Based on the Combination of Airborne LiDAR Data and Aerial Multispectral Images Using a Single-Tree Approach. Forests, 8:467.

Sačkov, I., Scheer, Ľ., Bucha, T., 2019a: Predicting forest stand variables from airborne LiDAR data using a tree detection method in Central European forests. Central European Forestry Journal, 65:191–197.

Sačkov, I., Kulla, L., Bucha, T., 2019b: A Comparison of Two Tree Detection Methods for Estimation of Forest Stand and Ecological Variables from Airborne LiDAR Data in Central European Forests. Remote Sensing, 11:1431.

Smreček, R., Sačkov, I., Michňová, Z., Tuček, J., 2017: Automated tree detection and crown delineation using airborne laser scanner data in heterogeneous East-Central Europe forest with different species mix. Journal of Forest Researche, 28:1049–1059.

Solberg, S., Næsset, E., Bollandsås, O. M., 2006: Single-tree segmentation using airborne laser scanner data in a structurally heterogeneous spruce forest. Photogrammetric Enginneering and Remote Sensing, 72:1369–1378.

Sparks, A. M., Corrao, M. V., Smith, A. M. S., 2022: Cross-Comparison of Individual Tree Detection Methods Using Low and High Pulse Density Airborne Laser Scanning Data. Remote Sensing, 14:3480.

Torresan, C., Carotenuto, F., Chiavetta, U., Miglietta, F., Zaldei, A., Gioli, B., 2020: Individual Tree Crown Segmentation in Two-Layered Dense Mixed Forests from UAV LiDAR Data. Drones, 4:10.

Vauhkonen, J., Ene, L., Gupta, S., Heinzel, J., Holmgren, J., Pitkänen, J. et al., 2012: Comparative testing of single-tree detection algorithms under different types of forest. Forestry, 85:27–40.

Vauhkonen, J., Maltamo, M., McRoberts, R. E., Næsset, E., 2014: Introduction to Forestry Applications of Airborne Laser Scanning. In: Maltamo, M., Næsset, E., Vauhkonen, J. (eds.): Forestry Applications of Airborne Laser Scanning: Concepts and Case Studies [Internet]. Dordrecht, Springer Netherlands, p. 1–16. Available from: https://doi.org/10.1007/978-94-017-8663-8_1.

Wang, Y., Hyyppä, J., Liang, X., Kaartinen, H., Yu, X., Lindberg, E. et al., 2016: International Benchmarking of the Individual Tree Detection Methods for Modeling 3-D Canopy Structure for Silviculture and Forest Ecology Using Airborne Laser Scanning. IEEE Transaction on Geoscience and Remote Sensing, 54:5011–5027.

Zaforemska, A., Xiao, W., Gaulton, R., 2019: Individual tree detection from UAV LiDAR data in a mixed species Woodland. International Archives of Photogrammetry and Remote Sensing, XLII-2-W13:657–63.

Zhang, Y., Wang, M., Mango, J., Xin, L., Meng, C., Li, X., 2024: Individual tree detection and counting based on high-resolution imagery and the canopy height model data. Geo-Spatial Information Science, 27:2162–2178.

Zhen, Z., Quackenbush, L. J., Zhang, L., 2016: Trends in Automatic Individual Tree Crown Detection and Delineation – Evolution of LiDAR Data. Remote Sensing, 8:333.

Other sources:

McGaughey, R., 2024: FUSION/LDV: Software for LIDAR Data Analysis and Visualization. 226 p.